

Asymmetry in attosecond streaking from a degenerate stateXiang-Ru Xiao,¹ Hao Liang,¹ Mu-Xue Wang,¹ Liang-You Peng,^{1,2,*} and Qihuang Gong^{1,2}¹*State Key Laboratory for Mesoscopic Physics and Collaborative Innovation Center of Quantum Matter, School of Physics, Peking University, Beijing 100871, China*²*Collaborative Innovation Center of Extreme Optics, Shanxi University, Taiyuan, Shanxi 030006, China*

(Received 29 May 2017; published 30 August 2017)

By the numerical solution to the time-dependent Schrödinger equation, we observe a remarkable asymmetry in the photoelectron streaking spectra when the He^+ ion is ionized by an attosecond pulse from the $2s$ state in the presence of a weak infrared pulse. An analytical theory based on the modified perturbation theory is developed to quantitatively account for the underlying mechanism. We find that a transition occurs between the degenerate $2s$ and $2p$ states under the influence of the infrared electric field before the arrival of the attosecond pulse. The observed asymmetry in the attosecond streaking is formed by the interference of photoelectrons ionized from the $2s$ and $2p$ states. Using the sensitivity of the asymmetry to the infrared (IR) electric field at the moment of attosecond photoionization, we show that the present finding provides a highly reliable way to fully characterize the IR waveform in the streaking experiment.

DOI: [10.1103/PhysRevA.96.023428](https://doi.org/10.1103/PhysRevA.96.023428)**I. INTRODUCTION**

Attosecond physics has been widely studied inside atoms and molecules [1,2], solid systems [3], and nanoscale structures [4] due to the development of advanced light sources such as attosecond laser pulses [5–10] and the well-controlled intense infrared laser [11,12]. A new age for the ultrafast sciences has been opened up to trace and control the electronic motion in the microscopic world. One of the most important technologies in attosecond science is the attosecond streak camera [13–15], which was initially proposed for the characterization of the attosecond extreme ultraviolet (xuv) pulse and the ultrashort infrared (IR) pulse by several retrieval algorithms [16–20]. Attosecond streaking has been since developed into a powerful tool to study many fundamental problems, such as photoionization time delay [21–27]. In addition, some other similar technologies based on attosecond streaking, in which the xuv pulse and IR pulse are employed as the pump or probe, are used to investigate the electronic dynamics in ultrashort processes [28–31].

In most of the previous streaking experiments, only the electron spectrum in the forward direction of the laser polarization has been utilized to extract the relevant observable for further analysis. This relies on the basic idea that the streaking field is too weak to perturb the system, so the distribution of photoelectrons should be symmetric along the laser polarization after one-photon ionization from the initial state. The only effect of the IR can be described in a classical picture: The freed electron is dragged by the IR electric field and gains an additional momentum $\Delta\mathbf{p} = -\int_{t_i}^{\infty} \mathbf{E}_{\text{IR}}(t') dt' = -\mathbf{A}_{\text{IR}}(t_i)$. As a result, only a shift on the momentum distribution occurs and the spectra in both the forward and backward directions look the same.

In this work, we report and analyze a hitherto unrecognized phenomenon caused by the IR field in attosecond streaking experiments: A substantial asymmetry is observed in the photoelectron distribution along the laser polarization for a de-

generate initial state. Many years ago, the transitions between degenerate states of excited hydrogen atoms were found in the collision processes [32–37]. To the best of our knowledge, this phenomenon has been scarcely discussed when the atom or molecule interacts with a laser field. Recently, the time delay in photoemission from spin-degenerate states of solids has been studied [38]. In the present work, when the hydrogenlike He^+ ion in the $2s$ state is employed in the numerical streaking experiment, we find that the resultant asymmetric distribution of photoelectrons is caused by a transition between the degenerate $2s$ and $2p$ states due to the IR electric field before the arrival of the attosecond pulse. An analytical theory based on the modified perturbation theory is developed to quantitatively describe the asymmetric phenomenon. We show that this effect is very sensitive to the vector potential at the time of attosecond photoionization and can be used to characterize the waveform of the IR field. Most importantly, it can easily be observed in streaking experiments for any other systems with degenerate levels.

II. RESULTS AND DISCUSSIONS

The numerical experiments are performed by solving the three-dimensional (3D) time-dependent Schrödinger equation (TDSE) for a hydrogenlike atom with a realistic Coulomb potential [29,39,40]. The differential distribution of the photoelectron with momentum \mathbf{p} is obtained by projecting the final wave function onto the scattering states of the same atomic system, i.e., $D(\mathbf{p}) = |\langle \psi_{\mathbf{p}}^{(-)} | \psi_f \rangle|^2$. In this work, both the length and the velocity gauge are employed to describe the laser-atom interaction. As depicted in the top panel of Fig. 1, the streaking configuration of the fields consists of a short xuv pulse and a weak few-cycle IR pulse, both linearly polarized along the z axis with a \sin^2 envelope. As examples, we show the streaked spectrum $D(\mathbf{p})$ in Figs. 1(a) and 1(b), respectively ionized from the $1s$ state of an H atom and the $2s$ state of a He^+ ion, by an eight-cycle xuv pulse with $\omega_{\text{xuv}} = 2$ a.u. and $I_{\text{xuv}} = 1 \times 10^{13}$ W/cm² in the presence of a two-cycle IR field with $\lambda_{\text{IR}} = 1000$ nm and $I_{\text{IR}} = 1 \times 10^{12}$ W/cm².

*liangyou.peng@pku.edu.cn

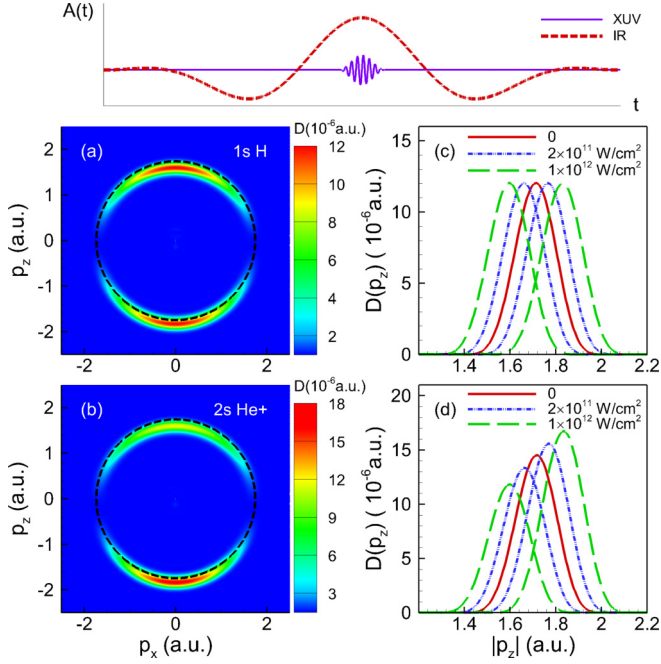


FIG. 1. The photoelectron momentum distribution $D(\mathbf{p})$ (left column) and $D(p_z)$ (right column) from (a), (c) the $1s$ state of H and (b), (d) the $2s$ state of He^+ from the attosecond streaking depicted in the top panel. In (a) and (b), $I_{\text{IR}} = 1 \times 10^{12} \text{ W/cm}^2$ and the dashed circle is a reference to the momentum shift. In (c) and (d), by making $|p_z|$ the abscissa, $D(p_z)$ are shown for both the forward and backward directions at three indicated intensities of I_{IR} .

Consistent with the classical picture of the streaking, $D(\mathbf{p})$ in Fig. 1(a) for the $1s$ state shows a perfect symmetry, merely with a downward shift caused by the IR field. On the contrary, for the $2s$ state in Fig. 1(b), one observes an obvious asymmetry of $D(\mathbf{p})$ in the forward and backward directions of the streaking field; i.e., more photoelectrons are ejected in the negative p_z . To see this asymmetry more clearly, we present in Figs. 1(c) and 1(d) the photoelectron distribution $D(p_z)$ along the axis

of the laser polarization, for the $1s$ state of H and the $2s$ state of He^+ , respectively, at different IR intensities. The spectra for the former case always show a symmetry at any I_{IR} , while the asymmetry for the latter case persists and increases as the increase of the IR intensity.

To uncover the underlying physics, we employ a single slowly varying pulse (SSVP) to replace the IR pulse, which allows us to develop an analytic and quantitative theory to identify the different roles played by the streaking field. The entire SSVP consists of the rising, the flat, and the falling parts, whose vector potential is respectively given by

$$A(t) = \begin{cases} A_0 \left(\frac{t}{\tau_0} - \frac{1}{2\pi} \sin \frac{2\pi t}{\tau_0} \right), & t \in [0, \tau_0] \\ A_0, & t \in [\tau_0, \tau_0 + \tau] \\ A_0 \left(1 - \frac{t''}{\tau_0} + \frac{1}{2\pi} \sin \frac{2\pi t''}{\tau_0} \right), & t'' \in [0, \tau_0], \end{cases} \quad (1)$$

where $t'' = t - (\tau_0 + \tau)$. For a given A_0 , the duration τ_0 should be sufficiently long to satisfy the condition of a slow variation so that the electric field $E(t) = -\frac{\partial}{\partial t} A(t)$ of the SSVP is weak enough not to induce a significant ionization, which mimics the typical requirement of attosecond streaking. In addition, the xuv pulse is placed in the flat part, as shown in the top panel of Fig. 2(a), where the total vector potential and electric field are plotted. This setting allows us to decouple the main steps of the physical processes. Taking $A_0 = 0.08 \text{ a.u.}$ and $\tau_0 = 2\tau = 55.2 \text{ a.u.}$, we show $D(p_z)$ in Fig. 2(a) from the $2s$ state of He^+ , calculated in both gauges. The xuv pulse is the same as that used in Fig. 1 and the value of 0.08 for A_0 here corresponds to the peak value of $A_{\text{IR}}(t)$ when $I_{\text{IR}} = 2 \times 10^{11} \text{ W/cm}^2$ in Fig. 1. As can be seen, one exactly reproduces the corresponding asymmetric distribution shown in Fig. 1(d) for the $2s$ state of He^+ in the usual attosecond streaking. However, if one chooses to switch off the rising or the falling part of the SSVP, the TDSE simulation in the length gauge will produce either a symmetric distribution with a momentum shift or an asymmetric distribution without a momentum shift, as shown in Figs. 2(b) and 2(c), respectively.

The above numerical experiments with the SSVP successfully help us identify two independent processes with different

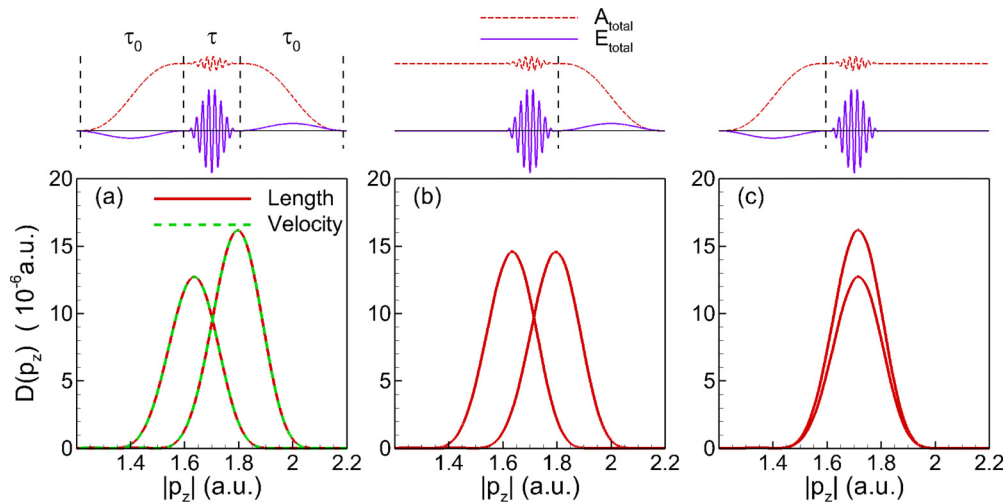


FIG. 2. (a) The streaking spectrum $D(p_z)$ calculated by the length and the velocity gauge in TDSE with the complete SSVP. The result from the length gauge calculation without (b) the rising part or (c) the falling part of the SSVP. Top: The total $A(t)$ and $E(t)$ for each respective case and the field parameters chosen so as to mimic one of the cases for the $2s$ state of He^+ , shown in Fig. 1(d).

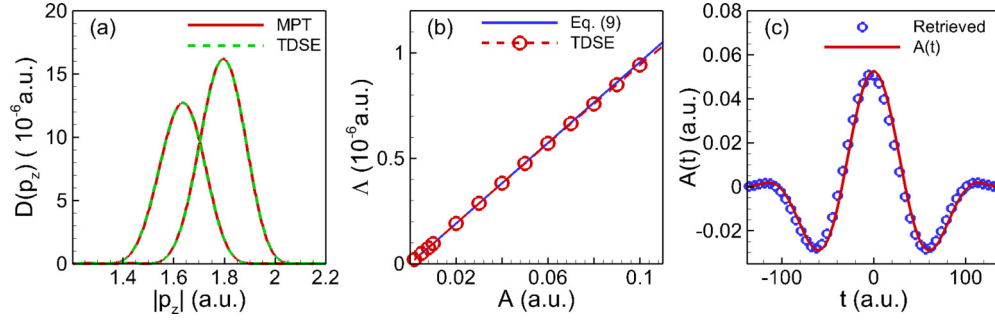


FIG. 3. (a) The same streaking spectra as in Fig. 2(a) calculated by the analytical theory [cf. Eq. (6)], compared with the TDSE result. (b) The asymmetric parameter extracted from the streaking spectrum and analytically calculated by Eq. (9) for the SSVP with various A_0 . (c) The vector potential of the few-cycle IR pulse used in Fig. 1 is accurately retrieved by using the asymmetric parameter from the streaking spectrum.

effects. Before the xuv arrives, the rising part will strongly interact with the initial $2s$ state, which leads to the resultant asymmetry of $D(p_z)$. After being ionized by the xuv pulse, the electron will be accelerated in a classical way by the falling part, which induces a momentum shift of the photoelectron. In order to seek the underlying mechanism leading to the observed differences between the results for the $1s$ state of H and $2s$ state of He^+ , one should focus on the role played by the streaking pulse before the arrival of the xuv pulse. We calculate the populations of nearby bound states in the length gauge and find that the degenerate $2p$ state of He^+ is significantly populated by the electric field of the rising pulse. A superposed state of the $2s$ and $2p$ states is thus ionized by the xuv pulse and subsequently shifted by the falling part of the streaking pulse, which explains the remarkable asymmetry in the resultant streaking spectrogram.

Our conjecture can be quantitatively confirmed by an analytical theory. The population transfer from the degenerate $2s$ to $2p$ states can be described by the first-order perturbation theory when the field is sufficiently weak, in which case the transition element is given by

$$\begin{aligned} M &= -i \int_{t_0}^t \langle \psi_f | U(t, t') V_{\text{int}} U(t', t_0) | \psi_i \rangle dt' \\ &= -i \int_{t_0}^t e^{i(E_f - E_i)t'} \langle \psi_f | V_{\text{int}} | \psi_i \rangle dt'. \end{aligned} \quad (2)$$

For the $2s$ and the $2p$ states, it is simplified to

$$\beta(t) = -i \int_{t_0}^t \langle 2p | E(t') z | 2s \rangle dt' = i [A(t) - A(t_0)] d_{2p,2s}, \quad (3)$$

with the dipole moment

$$d_{2p,2s} = \int R_{21} Y_{10}^* r \cos \theta R_{20} Y_{00} d\mathbf{r} = -\frac{3}{Z} = -\frac{3}{2}. \quad (4)$$

Equation (3) indicates that a transition between the $2s$ and $2p$ states will occur for a field with a nonzero accumulation of the vector potential. This process can be intuitively understood as an electron transfer from the $2s$ to the $2p$ state by absorbing one zero-energy photon. For a weak pulse or a SSVP, the electron can be hardly pumped to higher excited or continuum

states. Therefore, one can write the state at time t under the streaking field as

$$|\psi(t)\rangle = e^{iI_p t} [\sqrt{1 - |\beta(t)|^2} |2s\rangle + \beta(t) |2p\rangle], \quad (5)$$

where $I_p = -E_{2s} = -E_{2p} = 0.5$ a.u.

In the usual streaking setup, the bound electrons are pumped by the xuv pulse from the initial state to the laser dressed continuum state [41], in which the electronic wave packet is then controlled by the rest of the IR field. By using this idea in the current situation for the initial state given by Eq. (5), the final ionization amplitude can be analytically given by

$$\begin{aligned} M_{\mathbf{p}} &= -i \int_{t_0}^{t_f} dt' e^{iS_{\mathbf{p}}(t')} \langle \psi_{\mathbf{k}}^c | z | [\sqrt{1 - |\beta|^2} |2s\rangle + \beta |2p\rangle] \\ &= -i \int_{t_0}^{t_f} dt' e^{iS_{\mathbf{p}}(t')} E(t') [\sqrt{1 - |\beta|^2} d_{\mathbf{k},2s} + \beta d_{\mathbf{k},2p}], \end{aligned} \quad (6)$$

where $S_{\mathbf{p}}(t) = \int_{t_0}^t [(\mathbf{p} + \mathbf{A}(t'))^2/2 + I_p] dt'$, $d_{\mathbf{k},2s} = \langle \psi_{\mathbf{k}}^c | z | 2s \rangle$, $d_{\mathbf{k},2p} = \langle \psi_{\mathbf{k}}^c | z | 2p \rangle$, and $\mathbf{k}(t) = \mathbf{p} + \mathbf{A}(t)$. The Coulomb wave function $\Psi_{\mathbf{k}}(\mathbf{r}, t) = \langle \mathbf{r} | \psi_{\mathbf{k}}^c \rangle$ can be calculated numerically [42] and then the ionization amplitude (6) can be easily obtained by a numerical integration.

The above modified perturbation theory (MPT) successfully elucidates the two main effects in the streaking spectrum. First, using the Coulomb-Volkov state [43,44] as the final state can account for the shift of the momentum distribution, which can be seen from the variable substitution $\mathbf{k}(t) = \mathbf{p} + \mathbf{A}(t)$. Second, the asymmetry caused by the transition between the two degenerate states can be explained from the opposite parity of the $2s$ and $2p$ states. The dipole moment to the continuum state from the $2s$ state is antisymmetric along the laser polarization direction, while that for the $2p$ state is symmetric; i.e., $d_{\mathbf{k},2s} = -d_{-\mathbf{k},2s}$ and $d_{\mathbf{k},2p} = d_{-\mathbf{k},2p}$. The final photoelectron spectrum from both states will get a constructive interference in one direction and a destructive interference in the opposite direction. The streaking spectrum $D(p_z)$ for the SSVP along the z axis calculated by Eq. (6) is shown in Fig. 3(a), together with that from the TDSE calculation shown previously in Fig. 2(a). As one can see, the result of our analytical theory (MPT) is in excellent agreement with the exact one from the TDSE.

After uncovering the reasons for the observed asymmetry, we now address one of its potential applications to characterize the waveform of the streaking pulse. It is usually assumed that the vector potential of the streaking pulse barely changes during the short time window around t_i when the atom is ionized by the attosecond pulse. One can thus regard the vector potential $\mathbf{A}(t_i)$ as a constant. The difference between the ionization probabilities at two opposite final momenta $\mathbf{p}_\pm = \pm \mathbf{k} - \mathbf{A}$ can be shown to be

$$\begin{aligned} \Delta(\mathbf{k}) &= |M_{\mathbf{p}_-}|^2 - |M_{\mathbf{p}_+}|^2, \\ &\approx 4\sqrt{1 - |\beta|^2} |\beta| |d_{\mathbf{k},2s}| |d_{\mathbf{k},2p}| |\tilde{E}(\mathbf{k})|^2 \cos\left(\phi_{\mathbf{k}} - \frac{\pi}{2}\right), \\ &\approx 4|d_{2p,2s}| |d_{\mathbf{k},2s}| |d_{\mathbf{k},2p}| |\tilde{E}(\mathbf{k})|^2 \cos\left(\phi_{\mathbf{k}} - \frac{\pi}{2}\right) A, \end{aligned} \quad (7)$$

where $\phi_{\mathbf{k}} = \arg d_{\mathbf{k},2s} - \arg d_{\mathbf{k},2p}$ is the phase difference between the dipole moment for the $2s$ and the $2p$ states, and $\tilde{E}(\mathbf{k}) = \int_{t_0}^{t_f} dt' E(t') e^{ik^2 t'/2}$ is the Fourier transform of the electric field. In the last step of Eq. (7), we have kept only the first order of A . The analytical result tells us that the difference in opposite directions is proportional to the vector potential of the streaking field at the ionization time t_i , which agrees with our numerical observation shown in Fig. 1(d). One can further exploit this fact to retrieve the vector potential at t_i by reading off the asymmetry value from the streaking spectrum. For this, let us define an asymmetric parameter as the difference between the total ionization probability in opposite directions along the laser polarization,

$$\Lambda = \int_- |M_{\mathbf{p}_-}|^2 d\mathbf{p} - \int_+ |M_{\mathbf{p}_+}|^2 d\mathbf{p}, \quad (8)$$

which, by carrying out the integral of Eq. (7), can be analytically shown to be

$$\Lambda = \int \Delta(\mathbf{k}) d\mathbf{k} = 6KA, \quad (9)$$

with

$$K = \int |d_{\mathbf{k},2s}| |d_{\mathbf{k},2p}| |\tilde{E}(\mathbf{k})|^2 \cos(\phi_{\mathbf{k}} - \pi/2) d\mathbf{k}. \quad (10)$$

As a first example, the SSVP is used to test the above prediction. We calculate the streaking spectra at various values of A_0 and then extract the asymmetric parameter Λ . The result

from Eq. (9) is shown in Fig. 3(b), together with that extracted from the asymmetric spectrum $D(p_z)$ calculated by the TDSE. As expected, the asymmetric parameter linearly depends on the vector potential at the time of ionization when the streaking field is sufficiently weak, which coincides with the prediction by our MPT. Therefore, our finding provides an alternative way to characterize the waveform of the streaking IR pulse. In a well-studied system, such as hydrogenlike systems, the factor K can be numerically calculated accurately. Finally, we can confirm the reliability of our method by applying it to a realistic streaking setup as shown in Fig. 1. One can change the time delay between the attosecond pulse and the IR field and then extract the asymmetric parameter at each time delay from the streaking spectrum. The vector potential at the time of ionization can be retrieved from Eq. (9). As shown in Fig. 3(c), the vector potential of the IR field used in Fig. 1 is faithfully retrieved by our method.

III. CONCLUSIONS

In conclusion, for a degenerate initial state, we have observed a substantial asymmetry of attosecond streaking photoelectrons in the forward and backward direction of the laser polarization. By developing a quantitative theory, we identified a transition between the degenerate levels by the streaking IR field, and the resultant asymmetry was successfully explained by the interference of the photoelectrons from the opposite-parity degenerate states. By exploiting the sensitivity of the asymmetry to the IR vector potential at the time of the attosecond ionization, we have shown that our finding provides a reliable way to characterize the waveform of the streaking field. We emphasize that our method can significantly enhance the signal-to-noise ratio because the integration of the yield is used and it can be easily realized experimentally for any system with degenerate levels.

ACKNOWLEDGMENTS

This work is supported by the National Program on Key Basic Research Project of China (973 Program) under Grant No. 2013CB922402 and by the National Natural Science Foundation of China (NSFC) under Grant No. 11574010.

[1] F. Krausz and M. Ivanov, *Rev. Mod. Phys.* **81**, 163 (2009).
 [2] L.-Y. Peng, W.-C. Jiang, J.-W. Geng, W.-H. Xiong, and Q. Gong, *Phys. Rep.* **575**, 1 (2015).
 [3] S. Ghimire, G. Ndabashimiye, A. D. DiChiara, E. Sistrunk, M. I. Stockman, P. Agostini, L. F. DiMauro, and D. A. Reis, *J. Phys. B* **47**, 204030 (2014).
 [4] M. F. Ciappina *et al.*, *Rep. Prog. Phys.* **80**, 054401 (2017).
 [5] M. Hentschel, R. Kienberger, C. Spielmann, G. A. Reider, N. Milosevic, T. Brabec, P. Corkum, U. Heinzmann, M. Drescher, and F. Krausz, *Nature (London)* **414**, 509 (2001).
 [6] P. Agostini and L. F. DiMauro, *Rep. Prog. Phys.* **67**, 813 (2004).
 [7] G. Sansone *et al.*, *Science* **314**, 443 (2006).

[8] E. Goulielmakis *et al.*, *Science* **320**, 1614 (2008).
 [9] X. Feng, S. Gilbertson, H. Mashiko, H. Wang, S. D. Khan, M. Chini, Y. Wu, K. Zhao, and Z. Chang, *Phys. Rev. Lett.* **103**, 183901 (2009).
 [10] M. Chini, K. Zhao, and Z. Chang, *Nat. Photonics* **8**, 178 (2014).
 [11] T. Brabec and F. Krausz, *Rev. Mod. Phys.* **72**, 545 (2000).
 [12] *Few-Cycle Laser Pulse Generation and Its Applications*, Topics in Applied Physics, edited by F. X. Kärtner (Springer, Berlin, 2004), Vol. 95.
 [13] J. Itatani, F. Quéré, G. L. Yudin, M. Y. Ivanov, F. Krausz, and P. B. Corkum, *Phys. Rev. Lett.* **88**, 173903 (2002).

- [14] E. Goulielmakis, *Science* **305**, 1267 (2004).
- [15] R. Kienberger *et al.*, *Nature (London)* **427**, 817 (2004).
- [16] Y. Mairesse and F. Quéré, *Phys. Rev. A* **71**, 011401 (2005).
- [17] M. Chini, S. Gilbertson, S. D. Khan, and Z. Chang, *Opt. Express* **18**, 13006 (2010).
- [18] V. S. Yakovlev, J. Gagnon, N. Karpowicz, and F. Krausz, *Phys. Rev. Lett.* **105**, 073001 (2010).
- [19] C. Liu, M. Reduzzi, A. Trabattoni, A. Sunilkumar, A. Dubrouil, F. Calegari, M. Nisoli, and G. Sansone, *Phys. Rev. Lett.* **111**, 123901 (2013).
- [20] H. Wei, A.-T. Le, T. Morishita, C. Yu, and C. D. Lin, *Phys. Rev. A* **91**, 023407 (2015).
- [21] A. L. Cavalieri *et al.*, *Nature (London)* **449**, 1029 (2007).
- [22] M. Schultze *et al.*, *Science* **328**, 1658 (2010).
- [23] S. Nagele, R. Pazourek, J. Feist, K. Doblhoff-Dier, C. Lemell, K. Tkési, and J. Burgdörfer, *J. Phys. B* **44**, 081001 (2011).
- [24] R. Pazourek, S. Nagele, K. Doblhoff-Dier, J. Feist, C. Lemell, K. Tökési, and J. Burgdörfer, *J. Phys. Conf. Ser.* **388**, 012029 (2012).
- [25] R. Pazourek, J. Feist, S. Nagele, and J. Burgdörfer, *Phys. Rev. Lett.* **108**, 163001 (2012).
- [26] J. Su, H. Ni, A. Jaroń-Becker, and A. Becker, *Phys. Rev. Lett.* **113**, 263002 (2014).
- [27] R. Pazourek, S. Nagele, and J. Burgdörfer, *Rev. Mod. Phys.* **87**, 765 (2015).
- [28] J. Mauritsson, T. Remetter, M. Swoboda, K. Klünder, A. L’Huillier, K. J. Schafer, O. Ghafur, F. Kelkensberg, W. Siu, P. Johnsson, M. J. J. Vrakking, I. Znakovskaya, T. Uphues, S. Zherebtsov, M. F. Kling, F. Lépine, E. Benedetti, F. Ferrari, G. Sansone, and M. Nisoli, *Phys. Rev. Lett.* **105**, 053001 (2010).
- [29] M.-H. Xu, L.-Y. Peng, Z. Zhang, Q. Gong, X.-M. Tong, E. A. Pronin, and A. F. Starace, *Phys. Rev. Lett.* **107**, 183001 (2011).
- [30] J.-W. Geng, L.-Y. Peng, M.-H. Xu, and Q. Gong, *J. Phys. Conf. Ser.* **488**, 012003 (2014).
- [31] M. Kowalewski, K. Bennett, J. R. Rouxel, and S. Mukamel, *Phys. Rev. Lett.* **117**, 043201 (2016).
- [32] R. M. Pengelly and M. J. Seaton, *Mon. Not. R. Astron. Soc.* **127**, 165 (1964).
- [33] Y. N. Demkov, V. N. Ostrovskii, and E. A. Solov’ev, *Zh. Eksp. Teor. Fiz.* **66**, 125 (1974) [*Sov. Phys. JETP* **39**, 57 (1974)].
- [34] V. N. Ostrovskii and E. A. Solov’ev, *Zh. Eksp. Teor. Fiz.* **66**, 1590 (1974) [*Sov. Phys. JETP* **39**, 779 (1974)].
- [35] N. Toshima, *J. Phys. Soc. Jpn.* **42**, 633 (1977).
- [36] N. Toshima, *J. Phys. Soc. Jpn.* **43**, 605 (1977).
- [37] I. C. Percival and D. Richards, *J. Phys. B* **12**, 2051 (1979).
- [38] M. Fanciulli, H. Volfová, S. Muff, J. Braun, H. Ebert, J. Minár, U. Heinzmann, and J. H. Dil, *Phys. Rev. Lett.* **118**, 067402 (2017).
- [39] L.-Y. Peng, E. A. Pronin, and A. F. Starace, *New J. Phys.* **10**, 025030 (2008).
- [40] M. V. Frolov, D. V. Knyazeva, N. L. Manakov, A. M. Popov, O. V. Tikhonova, E. A. Volkova, M.-H. Xu, L.-Y. Peng, L.-W. Pi, and A. F. Starace, *Phys. Rev. Lett.* **108**, 213002 (2012).
- [41] M. Kitzler, N. Milosevic, A. Scrinzi, F. Krausz, and T. Brabec, *Phys. Rev. Lett.* **88**, 173904 (2002).
- [42] L.-Y. Peng and Q. Gong, *Comput. Phys. Commun.* **181**, 2098 (2010).
- [43] G. Duchateau, E. Cormier, and R. Gayet, *Phys. Rev. A* **66**, 023412 (2002).
- [44] V. D. Rodríguez, E. Cormier, and R. Gayet, *Phys. Rev. A* **69**, 053402 (2004).